J|A|C|S
COMMUNICATIONS

Published on Web 04/23/2004

Ultrastructure in Frozen/Etched Saline Solutions: On the Internal Cleansing of Ice

Fredric M. Menger,*,† Ashley L. Galloway,† Mary E. Chlebowski,† and Robert P. Apkarian‡

Department of Chemistry, Emory University, Atlanta, Georgia 30322, and Integrated Microscopy and Microanalytical Facility, Emory University, Atlanta, Georgia 30322

Received February 26, 2004; E-mail: menger@emory.edu

Over 70% of the earth's surface is covered by seawater having an average depth of 3.800 m. This water contains 3.5% dissolved salts (mainly sodium chloride). Malmgren[1] found that when seawater freezes, the salinity of the resulting sea ice depends on the rate of freezing. Sverdrup et al.[2] described formation of sea ice as a process that begins with isolated elongated crystals of pure ice forming a matrix that traps brine in separate cells. As the temperature drops, ice also forms in the cells, further concentrating the brine. If the temperature rises to about 0 °C, precipitated salts dissolve, the cells enlarge, the ice becomes porous, and the brine trickles down from the unsubmerged portions of the sea ice. The latter may then be fresh enough to melt into potable water. Worster and Wettlaufer[3] showed experimentally that brine drainage into underlying water occurs once the depth of the ice exceeds a critical value. The ice/brine ratio is an important variable of sea ice affecting its thermal, acoustic, electromagnetic, and mechanical properties.[3]

We have studied ice formation from saline, at concentrations near that of seawater, by cryo-etch high-resolution scanning electron microscopy (cryo-etch HRSEM). Surprising morphologies were thereby detected. But since cryo-etch HRSEM is a relatively new method,[4] and never before applied to frozen saline, we will first present some experimental details.

In a typical experiment, 10 μL of a 2−5 wt % aqueous NaCl solution was sandwiched between two gold planchettes. The sample was then loaded into a Balzers HPM 010 high-pressure freezer where liquid nitrogen was sprayed from two sides of a pressurized chamber (2.1 kbar). Freezing the sample from 20 to −105 °C took place in 5−6 ms (22000−25000 °C/s, consistent with the literature).[5] After freezing, the sample was immediately immersed in liquid nitrogen to maintain a temperature below −170 °C. Next, the sample was placed into a Gatan 3500 CT cryostage precooled to <−170 °C. A cold blade was then used to fracture the specimen and expose a fresh surface. Etching and coating of this surface were carried out after transferring the cryostage to a Denton DV-602 chromium coater where a vacuum of 2×10^{-7} Torr was maintained. Thus, the temperature was raised from −170 to −125 °C or −105 °C for time periods ranging from 5 to 120 min to allow exposed ice to vaporize by sublimation ("etching"). Once the etching was completed, the sample was cooled back to −170 °C and sputter-coated with chromium at a rate of 0.3 Å/s using a current and voltage of 50 mA and 300 V, respectively, under a 5×10^{-3} Torr atmosphere of argon.[6] The resulting 2-nm Cr film has the advantage of possessing smaller grain sizes than the precious metals. Finally, the sample was removed from the coater and transferred to a DS-130F field emission scanning electron microscope (beam diameter $\approx$ 1 nm) fitted with dual coldfinger anti-contamination traps and a Varian 860-cold-cathode gauge for monitoring the vacuum at the specimen. Images (4.8 MB), recorded in 16 s at −120 °C with a Pentium-based GW video capture board, were processed using Adobe Photoshop 6.0 as TIF files.

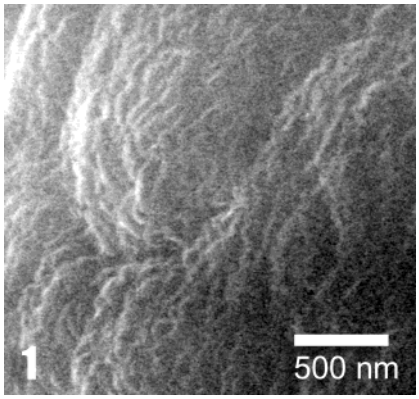

Figure 1. Doubly deionized water (18 mΩ) HPF from 20 °C and etched for 5 min at −105 °C.

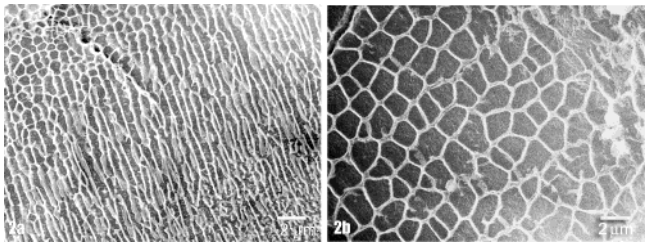

Figure 2. (a) NaCl, 2.0 wt % (HPF from 20 °C). (b) NaCl, 3.5 wt % (HPF from 20 °C). Samples were etched for 5 min at −105 °C.

It is necessary to explain briefly the merits of our high-pressure freezing (HPF). To avoid crystalline ice, which could obscure the salt morphologies in which we were interested, water was frozen at 2.1 kbar.[7] This pressure has three beneficial consequences: (a) the melting point of water drops from 0 to −22 °C, (b) homogeneous nucleation (supercooling) begins at −90 °C rather than −40 °C under atmospheric conditions, and (c) water viscosity increases 1500-fold. These features allow the easy attainment of microcrystalline or amorphous ice without the use of cryoprotectants. For comparison purposes we also plunge-froze 5-μL samples in liquid ethane (−183 °C), a method that also gives vitreous ice.[8]

When the cryo-etch HRSEM procedure was applied to salt-free water, only a coarsely textured amorphous ice was obtained (Figure 1). Electron micrographs of frozen saline also showed featureless ice in the absence of etching. Cryo-etch HRSEMs of 2 and 3.5 wt % NaCl, however, display a characteristic "fence-like" morphology (Figure 2). The samples had been high-pressure frozen from 20 °C with a 5-min etch at −105 °C (5000× magnification). Cells enclosed by the fences have sizes and shapes that depend on the rate of cooling. Plunge-freezing of 2 wt % NaCl from 20 °C and

† Department of Chemistry.
‡ Integrated Microscopy and Microanalytical Facility.

10.1021/ja040066k CCC: $27.50

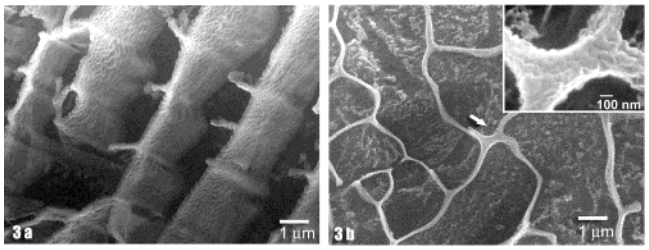

Figure 3. (a,b) NaCl, 2.0 wt %, plunged frozen in liquid ethane starting from 20 and 60 °C, respectively. Both samples were etched at −105 °C for 5 min.

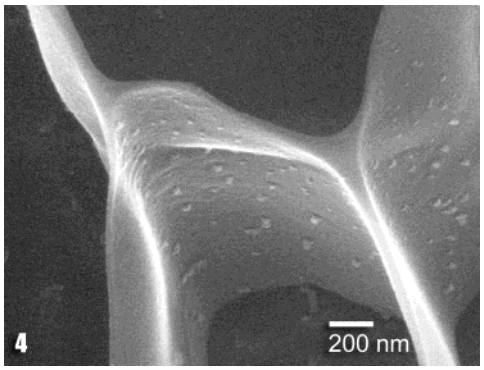

Figure 4. NaCl, 2 wt %, subjected to HPF and etched for 10 min at −105 °C.

60 °C to −183 °C produced larger fence-separated cells than seen with high-pressure freezing (Figure 3a and b, respectively).

It is well-known that, during cooling, certain materials, such as lava, experience thermal gradients that lead to propagating fragmentations.[9] Two observations mitigate against the partitions in Figures 2 and 3 being of this origin: (a) As seen in Figure 3a, the divisions are not cracks but walls of structured ice with a distinct depth to them. (b) And as seen in Figure 3b (upper right corner), there exists a granular morphology in a zone where four fences meet (arrow).

Despite the rapid cooling (5−6 ms with high-pressure freezing), patches of ice can at least partially cleanse themselves of salt by concentrating it in surrounding "fences". Since salt is strongly solvated, the fences survive the high-vacuum etching process whereas the enclosed amorphous ice does not. Walls of frozen brine, evident in Figure 3a, are the result. The fences become even more distinct when the etching time was increased from 5 to 10 minutes (Figure 4) to more thoroughly remove salt-associated ice that creates granular structures. The deep-etched fences are about 1−2 μm high and 10−50 nm thick.

When etching was carried out at −125 °C for 2 h after plunge-freezing at −183 °C, the surface appeared more heterogeneous, but fence-like structures were nonetheless evident (not shown). Cryo-etch HRSEM of 2 wt % Na_2SO_4, NH_4Cl, NaBr, and LiCl (5-min etch at −105 °C after high-pressure freezing) each gave unique morphologies (Figure 5). Aqueous LiCl, known from past work for its tendency to form amorphous ice,[10] displayed no segregation into fences when frozen.

The remarkably fast ability of water to free itself of dissolved salt during and/or after freezing can be understood from the structure of pure ice. Normal ice, that is to say, ice with which we are all familiar, is hexagonal and designated I_h.[11] Amorphous ice, a noncrystalline glass, can now be made in a variety of ways including vapor condensation at very low temperatures and so-called "hyperquenching" of 3−5 μm water droplets at 10^6−10^7 deg/s cooling rate.[12−14] In both cases water molecules are immobilized

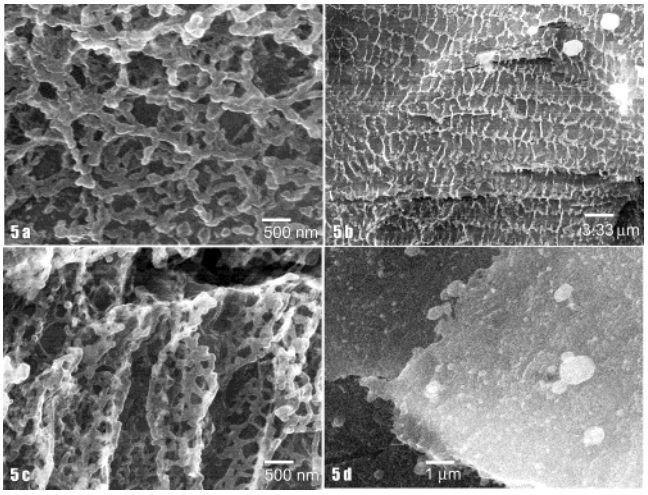

Figure 5. (a) Na_2SO_4, (b) NH_4Cl, (c) NaBr, (d) LiCl. See text for experimental details.

in a shorter time than is necessary for rearrangement into a crystalline state. Below −137 °C (referred to as the glass transition temperature, T_g), amorphous ice exhibits the mechanical properties of a solid with a microscopic structural disorder, ultrahigh viscosity (10^{13} Poise), and negligible rotational relaxation (10^3 s).[15] Above T_g, there occurs an onset of molecular rotation and conversion into a viscous liquid form of ice. It is important to realize that T_g is not an equilibrium transition temperature and that, being only quasi-thermodynamic, T_g may vary with experimental conditions.[16]

One of the most interesting aspects of amorphous ice is the appearance of metastable cubic ice, I_c, as the temperature is raised above −120 °C.[15,17,18] In the temperature range of −120 to −63 °C, cubic crystalline ice may coexist with the viscous liquid form of ice[19] (although there is debate on the exact fraction of each phase).[20] Ice I_c may possibly exist in the earth's high atmosphere,[21] while viscous liquid ice has been proposed to reside in subsurface layers of comets.[19]

Although information on frozen solutions of various salts is plentiful,[22−25] fence-like partitioning of amorphous ice after rapid freezing has not been reported. Barring the presence of saline fence structures in liquid water, their appearance in the cryo-etch HRSEM photographs can have only two origins: (a) The fences might form during the freezing process. If this is true, then water can divest itself of a salt at an extraordinary rate (as fast as 5−6 ms). (b) Alternatively, the migration of salt might occur within a few minutes during the etching procedure at −105 °C (32 °C above T_g). If this is true, then the bulk medium at −105 °C, composed of a "cubic ice/viscous liquid ice" composite, can obviously permit a remarkably effective saline-flow under the low-temperature conditions.

It was mentioned that, in the absence of etching, salt fences do not appear, nor are fences normally found in cryo-TEM where samples consist of thin, nonetched films. This does not prove that fences form during etching because the fences may be buried in ice and exposed only when the intervening ice is removed by sublimation. Yet saline-flow within the cubic ice/viscous liquid ice composite at −105 °C remains a distinct possibility. Cubic ice crystallites, if present at all, must be very small (i.e. <2 nm, the resolution of our electron microscope). Any channels that might conceivably be formed in the amorphous ice must also be below microscopic resolution. At present, therefore, we cannot exclude the presence of tiny channels, perhaps following contours of embedded submicroscopic I_c crystallites, which provide a route for saline drainage to the periphery of ice patches. (One is reminded here, on a much larger scale and slower time scale, of the behavior

of sea ice in nature). Consistent with this model, and our past experience with cryo-etch HRSEM on macromolecules where fences do not form, solutes can become too large, or diffuse too slowly, to traverse the narrow channels. Segregation into frozen walls of hydrated solute does not, therefore, occur. In this regard, surfactant micelles seem more similar to salt than to macromolecules.[26]

In summary, frozen 2−3.5% saline was investigated by cryo-etch high-resolution scanning electron microscopy. Thus, saline was either plunge-frozen in liquid ethane at −183 °C or else high-pressure frozen to −105 °C in 5−6 ms. Ice from a freshly exposed surface was then subjected to a high-vacuum sublimation ("etching"), a procedure that removes pure bulk ice in preference to ice from frozen hydrated salt. Granular icy "fences" were seen surrounding empty areas where amorphous ice had originally resided. The presence of such fences suggests that, during freezing, saline can purge itself of salt with remarkable speed (5−6 ms). Alternatively, channels (perhaps routed around submicroscopic crystallites of cubic ice (I_c) embedded in the amorphous ice at −105 °C) can guide the migration of salt to the periphery of ice patches. Aside from the fundamental interest of these results, salt morphologies are important to biologists who may encounter fences when examining buffered samples by cryo-etch methods.

Acknowledgment. This work was supported by the Army Research Office and an NIH equipment grant for the high pressure freezer.

References

(1) Malmgren, F. On the Properties of Sea Ice, Norwegian North Polar Expedition with the "Maud" 1918−1925. *Sci. Results* **1927**, *1*.
(2) Sverdrup, H. U.; Johnson, M. W.; Fleming, R. H. *The Oceans. Their Physics, Chemistry, and General Biology*; Prentice Hall: Englewood Cliffs, NJ, 1942.
(3) Worster, M. G.; Wettlaufer, J. S. *J. Phys Chem. B* **1997**, *101*, 6132−6136.
(4) Apkarian, R. P.; Wright, E. R.; Seredyuk, V. A.; Eustis, S.; Lyon, L. A.; Conticello, V. P.; Menger, F. M. *Microsc. Microanal*. **2003**, *9*, 286−295.
(5) Menco, B. P. M. *J. Elect. Microsc. Technol.* **1986**, *4*, 177−240.
(6) Apkarian, R. P. *Scanning Microsc.* **1994**, ***8***, 289−301.
(7) Moor, H. Theory and Practice of High-Pressure Freezing. In *Cryotechniques in Biological Microscopy*; Steinbrecht, R. A., Zierold, K., Eds.; Springer-Verlag: New York, 1987; Chapter 8.
(8) Ryan, K. P. *Scanning Microsc.* **1992**, *6*, 714−743.
(9) Jagla, E. A.; Rojo, A. G. *Phys. Rev. E* **2002**, *65*, 1−7.
(10) Elarby, A.; Jal, J. F.; Dupuy, J.; Chieux, P.; Wright, A.; Parreins, R. *J. Phys., Lett.* **1982**, *43*, L-355−L-363.
(11) Lekner, J. *Physica B* **1998**, *252*, 149−159.
(12) Hallbrucker, A.; Mayer, E.; Johari, G. P. *J. Phys. Chem.* **1989**, *93*, 7751−7752.
(13) Speedy, R. J. *J. Phys. Chem.* **1992**, *96*, 2322−2325.
(14) Bizid, A.; Bosio, L.; Defrain, A.; Oumezzine, M. *J. Chem. Phys.* **1987**, *87*, 2225−2230.
(15) Kivelson, D.; Tarjus, G. *J. Phys. Chem.* **2001**, *105*, 6620−6627.
(16) Williams, E.; Angell, C. A. *J. Phys. Chem*. **1977**, *81*, 232−237.
(17) Mayer, E.; Hallbruker A. *Nature* **1987**, *325*, 601−602.
(18) Johari, G. P.; Hallbrucker, A.; Mayer, E. *Nature* **1987**, *330*, 552−553.
(19) Jennishens, P.; Banham, S. F.; Blake, D. F.; McCoustra, M. R. S. *J. Chem. Phys.* **1997**, *107*, 1232−1241.
(20) Kohl, I.; Mayer, E.; Hallbrucker, A. *Phys. Chem. Chem. Phys.* **2000**, *2*, 1579−1586.
(21) Whalley, E. *Science* **1981**, *211*, 389−390.
(22) Grange B. W.; Viskanta, R.; Stevenson, W. H. *Int. J. Heat Mass Transfer* **1976**, *19*, 373−384.
(23) Tanner, J. E. *Cryobiology* **1975**, *12*, 353−363.
(24) Angell, C. A.; Sare, E. J. *J. Chem. Phys.* **1970**, *52*, 1058−1068.
(25) Chieux, P. *The Physics and Chemistry of Aqueous Ionic Solutions*; Bellissent-Funel, M. C., Nielson, G. W., Eds.; D. Reidel Publishing Co.: Dordrecht, 1987.
(26) Menger, F. M.; Zhang, H.; Caran, K. L.; Seredyuk, V. A.; Apkarian, R. P. *J. Am. Chem. Soc.* **2002**, *124*, 1140.

JA040066K